Cancer Chemother Pharmacol (2007) 60:891–897
DOI 10.1007/s00280-007-0436-5

ORIGINAL ARTICLE

Sonodynamic therapy on chemically induced mammary tumor: pharmacokinetics, tissue distribution and sonodynamically induced antitumor effect of gallium–porphyrin complex ATX-70

Nagahiko Yumita · Nobuo Okuyama · Kazuaki Sasaki · Shin-ichiro Umemura

Received: 17 October 2006 / Accepted: 31 January 2007 / Published online: 11 April 2007

Abstract Sonodynamically induced antitumor effect of a gallium porphyrin complex, ATX-70 was evaluated on a chemically induced mammary tumor in Sprague–Dawley rats. The timing of 24 h after the administration of ATX-70 was chosen for ultrasonic exposure, based on pharmacokinetic analysis of ATX-70 concentrations in the tumor, plasma, skin, and muscle. At an ATX-70 dose not less than 2.5 mg/kg and at a free-field ultrasonic intensity not less than 3 W/cm^2, the synergistic effect between ATX-70 administration and ultrasonic exposure on the tumor growth inhibition was significant. These results suggest that ATX-70 is a potential sonosensitizer for sonodynamic treatment of spontaneous mammary tumors.

Keywords Ultrasound · Chemically induced mammary tumor · Antitumor effect · Sonodynamic therapy · Pharmacokinetics

N. Yumita
School of Pharmaceutical Sciences, Toho University,
2–2–1 Miyama, Funabashi, Chiba 274–8510, Japan

N. Okuyama
School of Medicine, Toho University,
5–24–1 Oumori-nishi, Tokyo 274, Japan

K. Sasaki
Central Research Laboratory, Hitachi, Ltd,
1–280 Higashi-Koigakubo, Kokubunji,
Tokyo 185-8601, Japan

S. Umemura (✉)
School of Health Sciences, Faculty of Medicine,
Kyoto University, 53 Kawahara-cho,
Shogo-in, Sakyo-ku, Kyoto 606-8507, Japan
e-mail: sumemura@hs.med.kyoto-u.ac.jp

Abbreviations

PDT:	Photodynamic therapy
SDT:	Sonodynamic therapy
DMBA:	7,12-Dimethylanthracene
ATX-70:	7,12-Bis(1-decyloxyethyl)-Ga(III)-3,8,13, 17-tetramethyl-porphyrin-2,18-dipropionyl diaspartic acid

Introduction

Ultrasound has an appropriate tissue attenuation coefficient for penetrating intervening tissues to reach non-superficial objects while maintaining the ability to focus energy into small volumes. This is a unique advantage when compared to electromagnetic modalities such as laser beams in the application to non-invasive treatment of non-superficial tumors. Sonodynamic therapy (SDT) is a promising new concept of modality for cancer treatment using ultrasound. SDT is based on the local activation of a systemically administered sonosensitizer (sonochemical sensitizer) such as porphyrins by ultrasonic exposure [11, 12, 15, 16]. A mechanism for the sonodynamic activation of porphyrins attributing to the enhancement of active oxygen generation through acoustic cavitation was suggested [11, 20]. Among the metal–deuteroporphyrin complexes, which had been synthesized to be photosensitizers for photodynamic therapy, the gallium complexes showed the longest phosphorescence lifetime, much longer than hematoporphyrin (Hp) and its derivative (HpD) [8]. This long lifetime of the excited state can be a great advantage in the efficient generation of singlet oxygen through sonodynamic as well as photodynamic activations, assuming that basically the same energy transfer mechanism from the excited state is behind

them. Among such gallium porphyrin complexes, 7,12-bis(1-decyloxyethyl)-Ga(III)-3,8,13,17-tetramethylporphyrin-2,18-dipropionyl diaspartic acid, referred to as ATX-70 was found to show a significant antitumor effect when activated with ultrasound [1, 13, 17]. It enhanced ultrasonically induced cell killing much more efficiently than Hp and HpD [13]. These results demonstrated that ATX-70 has a potential as a sonosensitizer for tumor treatment with ultrasound.

Sonodynamic therapy using the combination of a certain porphyrin and ultrasonic exposure can be a synergistically-selective tumor-treatment modality, in which the side effects in surrounding normal tissues is minimized by the synergy between the molecular selectivity by the tumor-accumulative nature of porphyrins and the geometrical selectivity by localized ultrasonic exposure.

Sonodynamic antitumor effect has been evaluated using transplanted tumors [1, 6, 16–19]. They do not grow in the their native connective tissue matrix and do not fully mimic the human situation. It would be preferable therefore to evaluate the sonodynamic antitumor effects using a model system in which tumors grow in their own connective tissue matrix. The administration of 7,12-dimethylanthracene (DMBA) to a young female rat results in the formation of estrogen-dependent mammary tumors. It has been also reported that this mammary tumor developed in its own tissue matrix [2, 4]. This model has been widely used for evaluation of antitumor effect on mammary tumors since it resembles human breast cancer in its histology. It would be of interest to know whether the use of ATX-70 in combination with ultrasonic exposure is effective for treatment of this chemically induced mammary tumor.

In this study, in vivo effects of sonodynamic therapy with ATX-70 on the DMBA-induced mammary tumor were investigated using ultrasound at 2 MHz in a standing wave mode. In order to determine the optimum timing for ultrasonic exposure of the tumor, the time courses of ATX-70 concentrations in the plasma, mammary tumor, muscle, and skin were measured. The tumor was exposed to ultrasound at the time when the ATX-70 concentration in the tumor was at its maximum.

Materials and methods

Materials

7,12-bis(1-decyloxyethyl)-Ga(III)-3,8,13,17-tetramethylporphyrin-2,18-ipropionyl diaspartic acid (ATX-70) was supplied by Toyo Hakka Kogyo (Okayama, Japan). 7,12-dimethylanthracene (DMBA) was purchased from Sigma Chemical Company (St. Louis, MO, USA). All the other reagents were commercial products of analytical grade.

Tumor and animals

Female Sprague–Dawley rats (7 weeks old) were gavaged with 20 mg DMBA, dissolved in 2 ml sesame oil per rat. When the tumor grew to a diameter of about 10 mm, approximately 3 months after the administration of DMBA, the pharmacokinetic or treatment study was started. The experimental animals were treated according to the guideline proposed by the Science Council of Japan.

Determination of ATX-70 concentration in plasma and tissue

ATX-70 was dissolved in a sterilized saline solution and administered to the tumor-bearing rats at a dose of 5 mg/kg by intravenous injection from the caudal vein. Under pentobarbital anesthesia the blood samples were obtained from the femoral artery through a cannula to heparinized tubes 1, 5, 10, and 30 min, 1, 2, 6, 12, 24, 48, and 72 h after injection. Immediately after sampling, the blood was placed in a heparin-coated test tube and centrifuged at 2,500×*g* for 10 min to separate plasma. The tumor, liver, spleen, kidney, lung, heart, muscle, and skin were taken immediately after killing of the animals 2, 6, 24, 48, and 72 h after injection. The tissues were excised, blotted dry, and weighed. The samples were stored at –20°C until used. Plasma (0.1 ml) was mixed with 2.4 ml of 100 mM citric acid buffer (pH 3.0). A portion of tissue (0.1 g) was homogenized in 4.0 ml of the same buffer. Then the 2.5 ml plasma-buffer sample and the 2.5 ml of tissue-homogenate were each extracted with 5.0 ml of a chloroform: methanol mixture (1:1, v/v). After centrifugation at 3,000×*g* for 10 min, the chloroform layer was removed. The aqueous layer was shaken with 2.5 ml of chloroform for the second extraction. The first and the second chloroform layers were combined and evaporated to dryness in a water bath at 40°C. The residue was dissolved in 1.0 ml of a mobile phase for high-performance liquid chromatography (HPLC). After centrifugation at 2,500×*g* for 5 min, a 5-μl portion of the supernatant was injected into an HPLC system consisting of a pump (model L-6200, Hitachi, Tokyo, Japan), a fixed-loop injector (model 7125, Rheodine, Cotani, CA, USA), an analytic column (Wakocil 5C8, Wako Pure Chemical Ind., Osaka, Japan), a fluorescence detector (model F-1000, Hitachi, excitation: 405 nm, emission: 570 nm) and a data processor (model D-2500, Hitachi). The mobile phase was a mixture of methanol, water, and acetic acid (85:5:10, v/v/v).

Pharmacokinetic analysis

Pharmacokinetic analysis of plasma disappearance of ATX-70 was performed based on a two-compartment open model. The plasma concentration of ATX-70 ($C_p(t)$) is described by Eq. 1. The observed plasma concentrations were fitted to this equation and pharmacokinetic parameters, A, α, B, and β were determined by means of a non-linear least-squares method.

$$C_p(t) = A \cdot \exp(-\alpha \cdot t) + B \cdot \exp(-\beta \cdot t) \quad (1)$$

The area under the plasma concentration curve (AUC) from time zero to infinity, the plasma total body clearance (Cltot), and the distribution volume at the steady state (Vdss) were then calculated using the following equations.

$$AUC = A/\alpha + B/\beta \quad (2)$$

$$Cltot = Dose/AUC \quad (3)$$

$$Vdss = Dose(A \cdot \beta^2 + B \cdot \alpha^2)/(B \cdot \alpha + A \cdot \beta)^2 \quad (4)$$

The concentration of ATX-70 in tumor ($C_T(t)$) is given by the convolution integral equation:

$$C_T(t) = \int_0^t C_p(t-\theta) \cdot K_1 \exp(-k_2 t) d\theta \quad (5)$$

where K_1 is the transport clearance of ATX-70 to the tissue per unit volume of the tissue, the unit is min^{-1} (ml/h/ml) and k_2 is the first-order rate constant from the tissue to the plasma. To estimate K_1 and k_2 by means of the non-linear least squares method, the observed tissue concentrations ($C_T(t)$) were curve fitted to Eq. 5 in which C_P (t) was calculated from A,α, B, and β.

Ultrasonic exposure system

The ultrasonic exposure set-up is shown in Fig. 1. A piezoelectric ceramic disk transducer, 12 mm in diameter, was tightly bonded onto an aluminum-matching layer, which was cooled by circulating water to keep the transducer and tumor temperature below a certain level. The overall resonant frequency of the transducer was 1.92 MHz. Sine waves were generated by a wave generator (model MG442A, Anritsu, Tokyo, Japan) and amplified by an RF amplifier (model 210L, ENI, Rochester, NY, USA). The sinusoidal drive signal of the transducer was monitored with an oscilloscope during the exposure. A standing wave exposure mode was chosen for the relatively easy generation of reproducible cavitation. However, the output acoustic power from the transducer was calibrated in a free field (a progressive wave mode) to avoid difficulty in acoustic power estimation. The output acoustic pressure was measured in degassed water 30 mm from the transducer surface using a 1-mm-diameter polyvinylidene difluoride needle-type hydrophone (Medicoteknisk Institut, Denmark). Spatial average intensity was calculated by scanning the probe, for 4 mm axially and laterally, to eliminate the effect of ripples in the field due to Fresnel diffraction. The measured intensity was approximately proportional to the square of the peak-to-peak driving signal voltage of the transducer in the voltage range used for the exposure. In the in vivo ultrasonic exposure experiments, the transducer was driven at a voltage corresponding to a certain free-field intensity, which is used to specify the intensity of ultrasonic exposure in this paper.

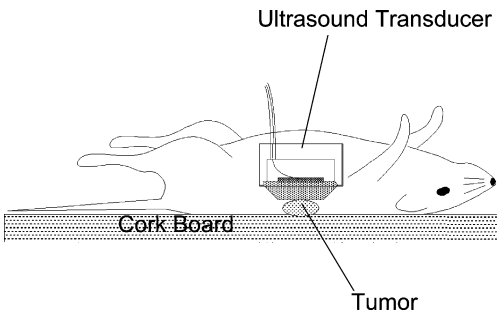

Fig. 1 Schematic diagram of ultrasonic exposure set-up. A cross section of the ultrasonic transducer is shown

Treatment protocol

The tumor bearing rats were divided into four groups of four rats: (1) the control group, and those treated with (2) ATX-70 alone, (3) ultrasound alone, and (4) ATX-70+ ultrasound. For the treatments with ATX-70, it was administered to a rat from the caudal vein. For the treatments with ultrasound, a rat was anesthetized with sodium pentobarbital (40 mg/kg, i.p.). The hair over the tumor was shaved and ultrasound gel was applied to the naked skin. The rat was fixed on a corkboard with the tumor upwards. The thermistor probe (Anritsu) was inserted into the tumor to monitor the temperature. The transducer was placed tightly on the tumor, which was exposed to ultrasound for 15 min. The transducer was cooled by circulating water at 25°C during the exposure to keep the temperature of the tumor below 35°C, which is much lower than the hyperthermia level. For the combined treatment, the tumor was exposed to ultrasound 24 h after ATX-70 administration.

Evaluation of antitumor effect

The length, width, and height (*a, b*, and *c* in mm) of the tumor were measured with a slide caliper every three days after treatment. The tumor volume was then calculated as

a × b × c/2. The mean and standard deviation (SD) were calculated for each group.

Results

Pharmacokinetics and tissue distribution

The concentrations of ATX-70 in the plasma after an intravenous administration are shown in Fig. 2. The observed data were best fitted by the bi-exponential equation (Eq. 1); the calculated pharmacokinetic parameters are listed in Table 1. The elimination half-life at the terminal phase ($t_{1/2\beta}$) was 8.3 h. The parameters that represent the distribution of ATX-70 to the tumor, skin, and muscle were calculated by using Eq. 5, and are shown in Table 2. The observed concentrations of ATX-70 in the tumor, skin, and muscle are plotted in Fig. 3. The fitted curves for the concentrations in tissues calculated with Eq. 5 and the parameters listed in Table 2 are also shown in Fig. 3.

The extraction ratios for the plasma, skin, muscle and tumor were 96, 81, 87, and 85%, respectively. The linearity between the HPLC peak area and the concentration was also confirmed in the observed concentration range.

The highest concentration of ATX-70 in the tumor was observed 24 h after administration. The ATX-70 concentration in the tumor exceeded by an order of magnitude that in the plasma 24 h or longer after the administration. The ATX-70 concentration in the tumor was significantly higher than those in the skin and muscle throughout the experiment.

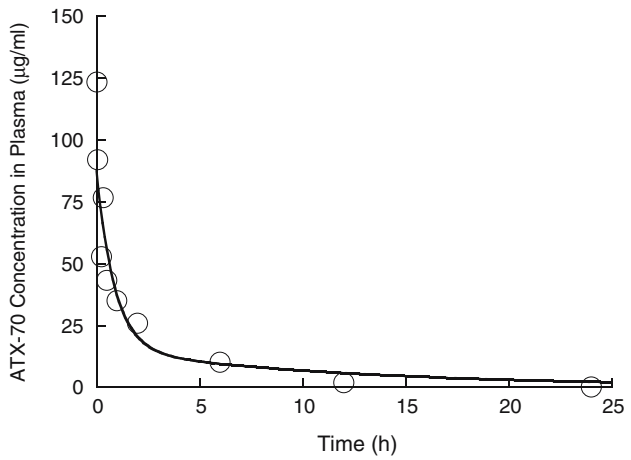

Fig. 2 Time course of ATX-70 concentration in plasma after intravenous administration. Each point and vertical bar represent the mean ± SD of four rats. The data are fitted with a bi-exponential curve

Sonodynamically induced antitumor effect

The effect of each treatment on the growth of the tumor is compared in Fig. 4 by plotting the tumor volume for 2 weeks after the day of the treatment. ATX-70 alone at a dose of 2.5 mg/kg had no inhibitory effect. Ultrasound alone at a free-field intensity of 3 W/cm^2 had no significant inhibitory effect, either. In contrast, ATX-70+ ultrasound at the same intensity showed such a significant antitumor effect that the tumor size started decreasing about a week after the treatment.

The effect of ultrasonic intensity on the tumor growth at a ATX-70 dose of 2.5 mg/kg is shown in Fig. 5. The five curves correspond to free-field ultrasonic intensities of 0, 1, 2, 3, and 5 W/cm^2, respectively. The ultrasound intensity threshold for the synergistic antitumor effect is clearly seen between the free-field intensities of 2 and 3 W/cm^2.

The effect of ATX-70 dose on the tumor growth at a free-field ultrasonic intensity of 3 W/cm^2 is shown in Fig. 6. The five curves correspond to ATX-70 doses of 0, 0.5, 1.0, 2.5, and 5.0 mg/kg, respectively. The synergistic antitumor effect became more and more significant as the ATX-70 dose increased.

No regrowth was observed in the tumors treated at an ultrasonic intensity not less than 3 W/cm^2 in combination at an ATX-70 dose not less than 2.5 mg/kg.

Discussion

Sonodynamic treatment, whose antitumor potential has been reported by several groups, is considered to be a promising therapeutic interventions for the treatment of malignant tumors. However, the sonodynamically induced antitumor effect of porphyrins has been evaluated mainly using implanted tumors. We employed a chemically induced tumor in rats to evaluate the antitumor effect of sonodynamic treatment. In the previous study we reported the effect of sonodynamic treatment with a sensitizer, HpD, with respect to histology [9] and tumor growth [20]. In this study we used ATX-70, a more efficient sonosensitizer than HpD, and investigated the effect of sonodynamic treatment with respect to its dependence on both ATX-70 dose and ultrasonic exposure intensity.

SDT of cancer is based on the use of a sonosensitizing agent that accumulates selectively in tumors and becomes cytotoxic when activated by ultrasonic exposure. It is reasonable to think that SDT is mostly effective if the tumor is exposed to ultrasound at the time when the ATX-70 concentration in the tumor is at its maximum. Furthermore, the adverse effects of treatments of SDT can be minimized by choosing the exposure timing when the sensitizer concentration in the tumor is significantly higher than that

Table 1 Pharmacokinetic parameters of ATX-70 after intravenous administration

Parameters	
A (μg/ml)	72.4 ± 6.3
B (μg/ml)	15.3 ± 3.1
α (h^{-1})	1.14 ± 0.09
β (h^{-1})	0.0831 ± 0. 003
Cltot (ml/h/kg)	10.7 ± 1.8
Vdss (ml/kg)	98.5 ± 14.5

Each value represents the mean ± SD of three rats

Table 2 Pharmacokinetic parameters of ATX-70 after intravenous administration

Parameters	Tumor	Muscle	Skin
K_1 ($\times 10^{-2}$ h^{-1})	1.79	0.65	0.54
k_2 ($\times 10^{-2}$ h^{-1})	3.19	38.1	53.2

Parameters were calculated from the mean tissue concentrations

in normal tissues [14, 16–19]. In order to determine the optimum timing for ultrasonic exposure, the concentration of ATX-70 in the plasma, tumor, muscle, and skin was measured and pharmacokinetically analyzed. The ATX-70 concentration in the plasma was well explained by the two-compartment open model. The distribution volume (Vdss) of ATX-70 was 93 ml/kg. This small value suggests that ATX-70 does not markedly distribute in tissues. The maximum concentration of ATX-70 in the tumor was observed 24 h after the administration. At the same time, the ATX-70 concentration in the tumor was several times higher than those in the plasma and in normal tissues such as the skin and muscle as shown in Fig. 3. On the basis of these results, we chose an ultrasonic exposure timing of 24 h after the intravenous administration of ATX-70.

The parameters calculated by using Eq. 5 in Table 2 represent the transport of ATX-70 to the tumor, skin, and muscle. The value of K_1 of tumor was 1/5 of β of plasma. This means that ATX-70 was transported to the tumor much slower than it was eliminated from the blood. The accumulation of porphyrin compounds in tumors has been reported in a variety of tumors of experimental animals and human beings. Recent *in vitro* and *in vivo* studies suggest the involvement of the low-density lipoprotein (LDL) receptor pathway as the mechanism of the accumulation of porphyrine compounds [3, 5, 7].

When both ATX-70 dose and ultrasonic exposure intensity are higher than certain levels, a significant anti-tumor effect was observed. At an ATX-70 dose not less than 2.5 mg/kg and at a free-field ultrasonic intensity not less than 3 W/cm^2, the synergistic effect between ATX-70 administration and ultrasonic exposure on the tumor growth inhibition was marked.

The ultrasonic intensity showed a relatively sharp threshold, which is typical for an ultrasonic effect mediated by cavitation. Ultrasonic cavitation is known to consist of two stages: (1) nucleation and growth of microbubbles under acoustic pressure, and (2) their sudden collapse. Sonochemical effects such as active oxygen generation are induced at the second stage, while the first stage requires ultrasonic intensity higher than the second stage. On account of the highly nonlinear acoustic nature of

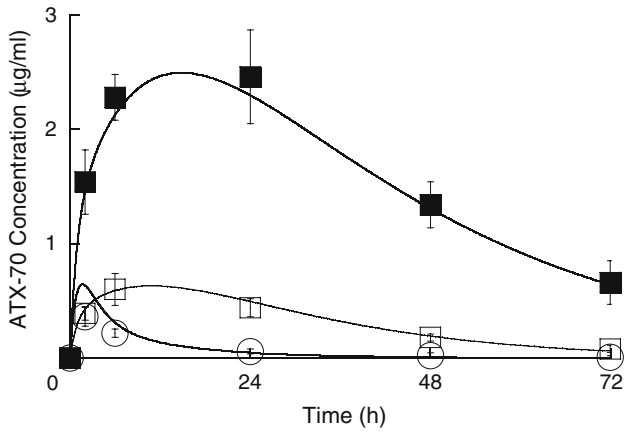

Fig. 3 Time course of ATX-70 concentration in tumor, skin, and muscle after intravenous administration. *Filled square* tumor; *open square* skin; *open circle* muscle. Each point and *vertical bar* represent the mean ± SD of four rats

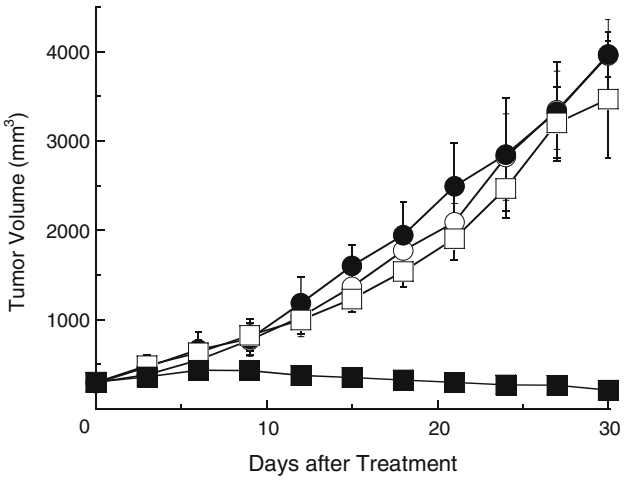

Fig. 4 Effect of ATX-70 and/or ultrasound on growth of chemically induced mammary tumor. *Open circle* control; *filled circle* ATX-70 alone; *open square* ultrasound alone; *filled square* ATX-70+ ultrasound. ATX-70 was administered 24 h before the treatment at a dose of 2.5 mg/kg and a free-field ultrasonic intensity of 3 W/cm^2 was used. Each point and vertical bar represent the mean ± SD of four rats

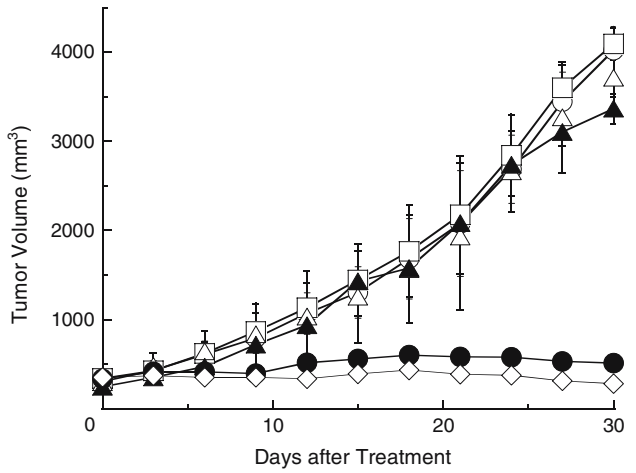

Fig. 5 Effect of ultrasonic intensity on tumor growth. ATX-70 was administered 24 h before the treatment at a dose of 2.5 mg/kg except for the control rats. *Open circle* control; *open square* a free-field ultrasonic intensity of 0; *open square* 1 W/cm^2; *filled triangle* 2 W/cm^2; *filled circle* 3 W/cm^2; *open diamond* 5 W/cm^2. Each point and *vertical bar* represent the mean ± SD of four rats

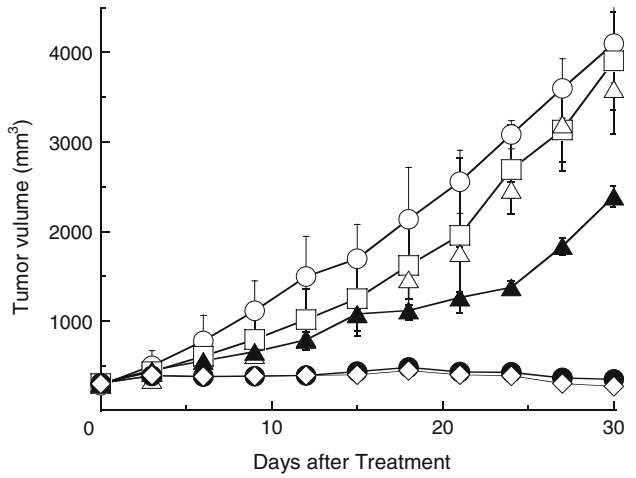

Fig. 6 Effect of ATX-70 dose on tumor growth. ATX-70 was administered 24 h before the treatment, and the tumor was exposed to ultrasound at a free-field intensity of 3 W/cm^2. *Open circle* Control; *open square*, ATX-70 dose of 0; *open square* 0.5 mg/kg; *filled triangle* 1.0 mg/kg; *filled circle* 2.5 mg/kg; *open square* 5.0 mg/kg. Each point and *vertical bar* represent the mean ± SD of four rats

microbubbles, ultrasonic cavitation shows a relatively sharp threshold in ultrasonic intensity, termed ‘‘cavitation threshold’’ [10].

The ATX-70 dose showed a broader threshold and the antitumor effect was gradually intensified as the dose increased. The observed effective dose of ATX-70 is at least an order of magnitude lower than its lethal dose [12]. Thus, as a potential adverse effect in the sonodynamic treatment with ATX-70, the toxicity of ATX-70 alone may be much less important than the potential photosensitive dermatitis. From this point of view, the considerable accumulation of ATX-70 in the tumor can be an advantage for the sonodynamic treatment using ATX-70 as a sensitizer.

Assuming that ATX-70 concentration in the tumor increases monotonously as the dose increases in the range of dose in this study, the observed synergistic antitumor effect can be regarded being highly dependent on the ATX-70 concentration in the tumor. Therefore, based on the presented results and the previously reported in vitro experimental results [5], it is thought that the observed in vivo cytotoxic effect may also be attributed to sonochemical activation of ATX-70. Due to the synergistic antitumor effect between ATX-70 and ultrasound at their proper doses, the average tumor size continued to decrease after the treatment.

In the tumors treated at both ultrasonic intensity and ATX-70 dose above the thresholds, no regrowth was observed. This could imply that the observed in vivo antitumor effect arose also from sonodynamically induced vascular shutdown in addition to the directly produced sonodynamic cytotoxicity. The vascular shutdown, sonodynamically induced with HpD, was pathologically observed and reported in our pervious paper [20]. From the ultrasonic intensity threshold, it is estimated that ultrasonic power in the order of 10 W is needed to sonodynamically treat a tumor 2 cm in diameter. When the tumor is not superficial, an order of magnitude higher input ultrasonic power may be needed to compensate the ultrasonic attenuation. This input power level is in the same order of magnitude with the basal metabolism of a human adult. If the ultrasonic focal spot is scanned over the tumor, the input power level can be significantly lowered in the expense of total treatment time.

In summary, the presented pharmacokinetic properties of ATX-70 in the tumor and normal tissues in combination with the presented sonodynamically induced inhibitory effect on the tumor growth suggest that ATX-70 is a potential sonosensitizer for the treatment of spontaneous mammary tumors. The results reported in this paper are experimental, but they significantly support the possibility of sonodynamic treatment using ATX-70. In future studies, experiments with focused ultrasound rather than plane waves, demonstrating its spatial selectivity by using animals in a size closer to human such as rabbits, need to be performed. The relatively sharp threshold in ultrasonic intensity will enhance the spatial selectivity in sonodynamically producing cytotoxicity in tissues. In this way, the synergy between the molecular selectivity of the sonosensitizer and the spatial selectivity of focused ultrasound will be achieved so as to suppress the adverse effect, which may otherwise take place in tissues out of the region to be treated.

References

1. Abe H, Kuroki K, Tachibana K, Awasthi A, Ueno A, Matsumoto H, Imakiire T, Yamauchi Y, Yamada H, Ariyoshi A, Kuroki M (2002) Targeted sonodynamic therapy of cancer using a photosensitizer conjugated with antibody against carcinoembryonic antigen. Anticancer Res 22:1575–1580
2. Agarwal R, Athar M, Elmets CA, Bickers DR, Mukhtar H (1990) Photodynamic therapy of chemically- and ultraviolet B radiation-induced murine skin papillomas by chloroaluminum phthalocyanine tetrasulfonate. Photochem Photobiol 56:43–50
3. Bellnier DA, Ho YK, Panday RK, Missert JR, Dougherty TJ (1989) Distribution and elimination of Photofrin II in mice. Photochem Photobiol 50:221–228
4. Brueggemeier RW, Li PK (1990) Effects of the aromatase inhibitor 7 alpha- (4′-amino) phenylthio-4-androstene-3, 17-dione on 7,12-dimethylbenz (a) anthracene-induced mammary carcinoma in rats. Cancer Res 48:6808–6810
5. Dougherty TJ (1993) Photodynamic therapy. Photochem Photobiol 58:895–905
6. Jin ZH, Miyoshi N, Ishiguro K, Umemura S, Kawabata K, Yumita N, Sakata I, Takaoka K, Udagawa T, Nakajima S, Tajiri H, Ueda K, Fukuda M, Kumakiri M (2000) Combination effect of photodynamic and sonodynamic therapy on experimental skin squamous cell carcinoma in C3H/HeN mice. J Dermatol 27:294–306
7. Kessel D (1986) Porphyrin-lipoprotein association as a factor in porphyrin loacatization. Cancer Lett 33:183–188
8. Nakajima S, Maeda T, Omote Y, Hayashi H, Yamazaki K, Kobo Y, Takemura S, Shindo Y, Sakata I (1989) Tumor localizing Ga–porphyrin complex (ATX-70) as a new photosensitizer excited with YAG-laser. J Jpn Soc Laser Med 10:225–228
9. Okuyama N, Sasamoto S, Kato N, Takagi K, Yamazaki S, Tsujimoto S, Yumita N, Nishigaki R, K.Sasaki, Umemura S (2000) The effect of sonodynamic therapy on rat mammary cancer (in Japanese). J Med Ultrasonics 27:1465–1469
10. Roy RA, Atchley AA, Crum LA, Fowlkes JB, Reidy JJ (1985) A precise technique for the measurement of acoustic cavitation thresholds and some preliminary results. J Acoust Soc Am 78:1799–1805
11. Umemura S, Yumita N, Nishigaki R, Umemura K (1990) Mechanism of cell damage by ultrasound in combination with hematoporphyrin. Jpn J Cancer Res 81:962–966
12. Umemura K, Yumita N, Nishigaki R, Umemura S (1996) Sonodynamically induced antitumor effect of pheophorbide a. Cancer Lett 102:151–157
13. Umemura S, Yumita N, Nishigaki R (1993) Enhancement of ultrasonically induced cell damage by a gallium–porphyrin complex, ATX-70. Jpn J Cancer Res 84:582–588
14. Umemura S, Sasaki K, Kawabata K (1995) Reduction of threshold for producing sonodynamic tissue damage by second-harmonic superimposition. In: Proceedings of 1995 IEEE ultrasonics symposium, pp 1567–1570
15. Yumita N, Nishigaki R, Umemura K, Umemura S (1989) Hematoporphyrin as a sensitizer of cell damaging effect of ultrasound. Jpn J Cancer Res 80:219–222
16. Yumita N, Nishigaki R, Umemura K, Umemura S (1990) Synergetic effect of ultrasound and hematoporphyrin on sarcoma 180. Jpn J Cancer Res 81:304–308
17. Yumita N, Sasaki K, Umemura S, Nishigaki R (1996) Sonodynamically induced antitumor effect of a gallium–porphyrin complex, ATX-70. Jpn J Cancer Res 87:310–316
18. Yumita N, Umemura S (2000) Sonodynamic therapy with photofrin II on AH130 solid tumor. Pharmacokinetics, tissue distribution and sonodynamic antitumoral efficacy of photofrin II. Cancer Chemother Pharmacol 51:74–78
19. Yumita N, Nishigaki R, Sakata I, Nakajima S, Umemura S (2000) Sonodynamically induced antitumor effect of 4-formyloximethylidene-3-hydroxy-2-vinyl-deuterio-porphynyl(IX)-6,7-diaspartic acid (ATX-S10). Jpn J Cancer Res 91:255–260
20. Yumita N, Okuyama N, Sasaki K, Umemura S (2004) Sonodynamic therapy on chemically induced mammary tumor: pharmacokinetics, tissue distribution and sonodynamically induced antitumor effect of porfimer sodium. Cancer Sci 95:765–769